Available online at www.sciencedirect.com

ScienceDirect

Energy Procedia 114 (2017) 37 – 45

Energy Procedia

13th International Conference on Greenhouse Gas Control Technologies, GHGT-13, 14-18 November 2016, Lausanne, Switzerland

Palladium (Pd) membranes as key enabling technology for pre-combustion CO_2 capture and hydrogen production

T.A. Peters[a,*], P.M. Rørvik[a], T.O. Sunde[a], M. Stange[a], F. Roness[b], T.R. Reinertsen[b], J.H. Ræder[a], Y. Larring[a], R. Bredesen[a]

[a]*SINTEF Materials and Chemistry, P.O. Box 124 Blindern, N-0314, Oslo, Norway*
[b]*Reinertsen AS, P.O. Box 6380 Sluppen, N-7492 Trondheim, Norway*

Abstract

Palladium (Pd) membranes are a promising enabling technology for power generation and hydrogen production with CO_2 capture. SINTEF has developed and patented a flexible technology to produce Pd-alloy membranes that significantly improves flux and thereby reduces material costs. Reinertsen AS and SINTEF aim to demonstrate the Pd membrane technology for H_2 separation on a side stream of the Statoil Methanol Plant at Tjeldbergodden, Norway. In the present article, we present the upscaling of the membrane manufacturing process, together with the membrane module and skid design and construction.

Peer-review under responsibility of the organizing committee of GHGT-13.

Keywords: Pre-combustion CO_2 capture; Palladium membrane upscaling; Industrial site hydrogen separation; Hydrogen.

1. Introduction

Dense Pd-based H_2-selective membrane technology is a very promising technology to reduce CO_2 emissions in the power and energy-intensive industrial sectors. Integrated in a combined power cycle, this membrane technology enables the efficient conversion of fossil fuel in large-scale power and hydrogen production with efficient capture of CO_2 [1-5]. In a natural gas fuelled pre-combustion decarbonisation (PCDC) cycle, the membranes can either be

* Corresponding author. Tel.: +47 982 43 941.
E-mail address: thijs.peters@sintef.no

Peer-review under responsibility of the organizing committee of GHGT-13.
doi:10.1016/j.egypro.2017.03.1144

integrated in the steam reforming (SR) or water-gas-shift process (WGS). From techno-economic assessments, however, it is favorable with respect to cost of CO_2 avoided/captured to integrate the membrane separation with the WGS process [6]. A main reason for this lies in the limited partial pressure of hydrogen in the steam reforming process at high pressure, resulting in a low driving force for the separation of hydrogen and consequently a high required membrane surface area. Furthermore, WGS reactors allow for lower membrane operation temperatures benefiting membrane stability, and a broader application range that also includes synthesis gas from gasification of coal and biomass. For natural gas, process design studies show that the membrane SR (M-SR) and the membrane WGS (M-WGS) process cycles have power generation efficiencies of 46.2% and 47.1%, respectively [7]. Even though the membrane technology is able to capture virtually 100% of CO_2, both cycles have been designed to operate at 92% capture due to economic benefits. Compared to competing carbon capture technologies, including chemical looping, sorbent and solvent-based processes, the M-WGS process has the highest efficiency and lowest CO_2 capture and avoidance cost potential [6, 8-11]. Fig. 1 illustrates the natural gas fuelled pre-combustion decarbonisation (PCDC) cycle with integrated M-WGS separation.

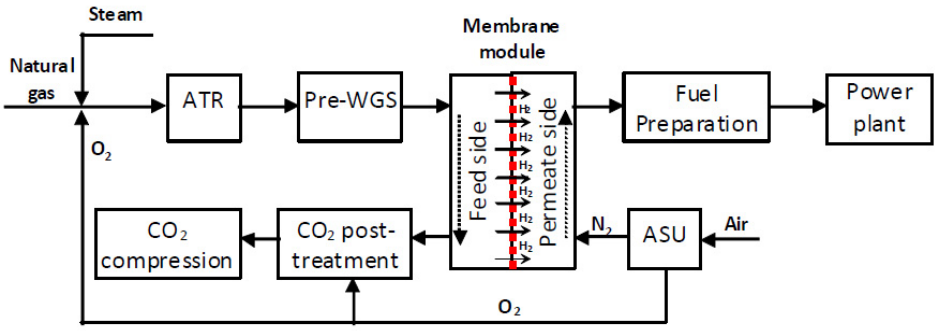

Fig. 1. Simplified system schematic of a natural gas fired power plant with an integrated membrane WGS reactor (M-WGS) for CO_2 capture.

Natural gas, mixed with steam and oxygen from an air separation unit (ASU), is fed to an autothermal reformer (ATR). The resulting syngas is fed to the M-WGS process. The sweep gas consists of compressed nitrogen from the ASU and/or steam enhancing the H_2 permeation through the membrane. The remaining stream contains mainly CO_2, steam and some non-recovered H_2. Subsequent condensation of the steam leaves concentrated CO_2 at high pressure, reducing the compression energy for transport and storage. The membrane technology is also relevant for the production of hydrogen as a decarbonised fuel for many applications, such as boilers, furnaces, engines and fuel cells. Currently, Tokyo Gas has demonstrated the world's largest scale Pd membrane natural gas reformer with a rated H_2 production capacity of 40 Nm^3/h (150 kW_{th}) and very high hydrogen production efficiency (HHV) of 81.4% [12]. In parallel with the process integration studies, large experimental efforts have tremendously progressed this technology forward, which is now positively perceived by industrial actors for scale-up and demonstration [3, 13].

SINTEF has developed and patented a flexible technology to produce Pd-alloy membranes with thickness down to 1-2 µm that significantly improves flux and thereby reduces material and capital costs. Differently from the common direct deposition onto the support, a so-called two-step process is employed [14, 15]. In the first step a thin defect-free Pd-alloy film is prepared by magnetron sputtering deposition onto a 'perfect surface' of a silicon wafer. In a second step the film is removed from the wafer and subsequently used self-supported or integrated with various supports of different pore size, geometry and size [16]. Currently, Reinertsen AS and SINTEF are involved in a GASSNOVA project aiming to demonstrate the membrane technology for H_2 separation on a side stream of the Statoil Methanol Plant at Tjeldbergodden, Norway. In the present article, we present the upscaling of the SINTEF two-stage Pd-alloy membrane manufacturing process that is currently on-going.

2. Membrane fabrication

2.1. Upscaling of Pd-alloy film deposition

Previous lab-scale sputtering to produce unsupported Pd-alloy membrane films using a CVC 601 magnetron sputtering system applied silicon single crystal substrates with size 4" and 6" as sacrificial substrate [17]. In the current upscaling effort we use a newly installed semi-industrial magnetron sputtering system (BVE3F system, Thin Film Equipment (TFE), Italy), Fig. 2, that allows for the deposition of Pd-alloy films with size 55×30 cm^2. The silicon substrates were replaced by glass substrates to allow for the larger size. The typical thickness applied in the current work of around 4 μm was obtained after a sputtering deposition time of approximately 3 h for the Pd-23%Ag alloy used as membrane film.

Fig. 2. TFE BVE3F magnetron sputtering system allowing for an up-scaled fabrication of Pd-alloy film.

2.2. Membrane manufacturing

In lab-scale membrane manufacturing, small strips of the Pd-alloy film were removed manually from the Si-substrate and wrapped along a tubular porous stainless steel membrane support in a helix-like manner. This production method has no limitation in terms of membrane length as subsequent films wrapped around the tubes are sealed by interdiffusion in the overlapping regions of the film [18]. Alternatively, larger rectangular sheets of free-standing Pd film are wrapped once around the tubular support with some overlap. This decreases the total length of overlap region per membrane length, and decreases the probability for leakage paths in the membrane. For upscaled production, free-standing films of 50 cm were wrapped on tubular porous 316L stainless steel supports. Sealing at the end-connectors was obtained by physical clamping. For this a semi-automated machine for film delamination and application on the membrane support was developed. The Pd-alloy film was typically wound 1.5 times around the porous tubular support to allow enough area for bonding between the first and second film layers. This results in an effective Pd membrane thickness of approximately 6 μm. The active membrane area available for permeation equals ~359 cm^2 per membrane. With the two-stage production method, thinner membrane films can be obtained, and down to 1-2 μm have conventionally been prepared on smaller scale [19, 20].

2.3. Membrane performance verification

The tubular-supported Pd-alloy membranes were tested in a unit designed and constructed for high-pressure membrane performance testing of up to 18 membranes simultaneously (~0.65 m^2 active membrane area). The membranes were placed inside a 316L stainless steel module (inside diameter 25 cm, Fig. 3), which was placed in a large vertical split furnace (Entech, Sweden) with a heated length of 80 cm. Automated mass flow controllers (Bronkhorst High-Tech) were used to control the gas supply of N_2 (5.0) and H_2 (5.5) to the membrane module. The

pressure was controlled with the help of a back pressure controller (Bronkhorst High-Tech). No active sweep was applied on the inside of the membrane tubes. When heating up the module, the module was kept in a N_2 atmosphere until 300°C was reached, then H_2 was introduced. A system of VICI stream selectors (Valco Instruments Co., Inc., USA) was used to monitor the performance of individual membranes. The flux of the respective gaseous components was calculated from the measured absolute permeate flow and the permeate composition measured by a micro GC (Agilent 490, USA). As this unit is limited in terms of feed flow rate per membrane area applied (50 $L \cdot min^{-1}$ for a total area of 0.65 m^2), it was primarily used to assess the membrane quality in terms of a low leakage. In addition, we have operated shorter membrane samples (typically ~150 cm^2 active membrane area) in a separate unit employing feed flow rates representative for real conditions (absolute flow up to 10 $L \cdot min^{-1}$, which equal feed flow rates up to 50 $Nm^3 \cdot m^{-2} \cdot h^{-1}$).

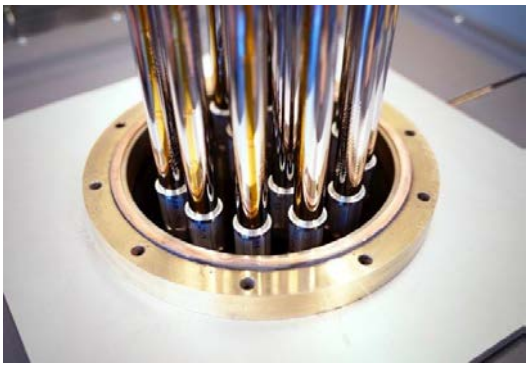

Fig. 3. Placement of membranes while lowering into the high pressure stainless steel module.

3. Results and discussion

3.1. Pd-alloy film preparation

Fig. 4 shows a Pd-23%Ag films deposited on 4" and 6" silicon wafers and on a 55×30 cm^2 glass substrate, respectively. The films that were sputtered on glass have a similar microstructure as the ones deposited on silicon wafers. Films of 55×30 cm^2 size produced in clean room to avoid detrimental effect of dust particles were easily delaminated from the glass. Under this conditions, Pd-alloy films were routinely produced with most films showing no detectable holes when shining light through from the backside on a light table.

Fig. 4. Photograph showing a Pd-23%Ag film applied on 4" and 6" silicon wafers and a 55×30 cm^2 glass substrate.

3.2. Membrane preparation

Fig. 5 shows a selection of membranes prepared. As seen in the figure, virtually all produced membranes had some wrinkles at parts of the membrane due to the challenge of winding the rectangular film evenly and tightly onto the support. It was found necessary to use straightened tubular supports for the membranes as slightly bent supports gave more wrinkling. Further improvements of the production method is in progress to reduce the amount of wrinkling in order to reduce the risk of leakage. The helix-like production method described above is in principle better for obtaining wrinkle-free membranes, but requires more efforts for scaling up production. Although most produced membranes showed some wrinkles, the amount of wrinkles was significantly reduced, and only observed in the overlap area after the membrane performance verification in pressurized hydrogen at high temperature. In the area with only one layer of Pd-alloy film, the large pressure difference applied has typically deformed the Pd–23%Ag film to follow the surface topography of the stainless steel support.

Fig. 5. Photograph showing six Pd–23%Ag/stainless steel composite membranes manufactured by SINTEF with permeable dimensions of 1 inch OD and 18 inch length.

3.3. Membrane performance verification

For deployment of the Pd-alloy membrane technology in CO_2 capture processes, preliminary process calculations have suggested a needed H_2/CO_2 separation factor of 100 in order to obtain a CO_2 capture rate above 90% [21]. In relation to absolute H_2 flux values obtained under realistic hydrogen recovery factors (HRF) of around 15 $Nm^3 \cdot m^{-2} \cdot h^{-1}$, one would thus allow leakage rates of up 0.5-1 $mL \cdot cm^{-2} \cdot min^{-1}$ under high operating pressures while still maintaining a H_2 purity above 98%. Fig. 6 shows a the obtained N_2-leakage flux through 5 membrane samples as a function of operating time and applied feed pressure. This initial test is performed to initiate the bonding of underlying Pd-alloy films, and to assess the membrane quality in terms of a low leakage.

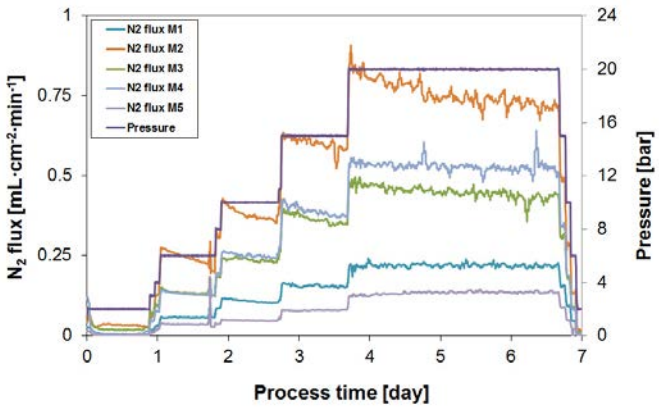

Fig. 6. N_2-leakage flux obtained during the initial bonding and quality verification of 5 membranes operated simultaneously, T ~365 °C, 40% H_2 in N_2 feed at a flow rate of 10 $NL \cdot min^{-1}$.

With increasing feed pressure the N_2 leakage increases. However, at each pressure level, the initial leakage increase is followed by a gradual decrease over time, which shows the result of the diffusion bonding occurring between overlapping films. The operation at 20 bars for a period of 3.5 days shows as well that the membranes are stable. Most of the membranes that are made show a leakage flux below 1 $mL \cdot cm^{-2} \cdot min^{-1}$ at 15 bars. Further improvements in application method of the free-standing Pd-alloy film onto the tubular support are expected to reduce the membrane leakage flux.

Fig. 7 shows the membrane performance as function of realistic operating conditions of feed flow rate per membrane area and feed pressure in a feed mixture containing either 50% H_2 (a) or 30% H_2 (b) in N_2, respectively. No active sweep was applied during these measurements. The membrane sample that is applied in this experiment shows a N_2 leakage flux of 0.4 $mL \cdot cm^{-2} \cdot min^{-1}$ at operating temperature and 15 bar. This is representative for the larger membrane samples produced, and agrees well with short lab-scale membranes prepared earlier [19].

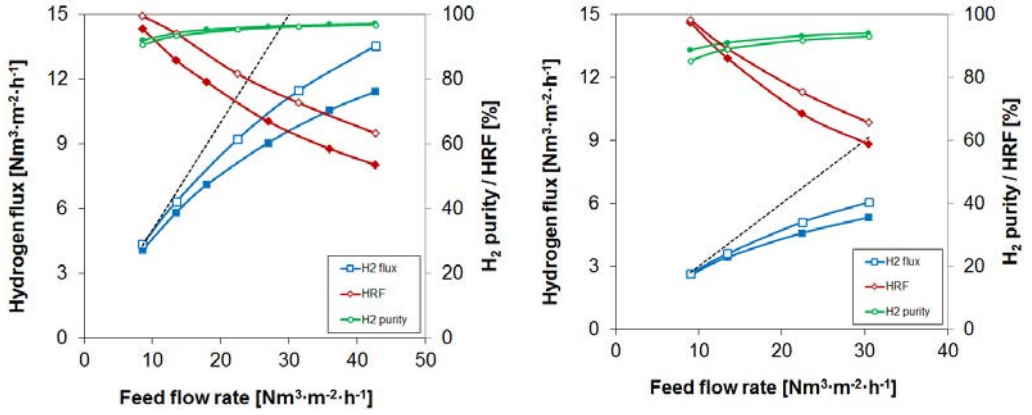

Fig. 7. Membrane performance as function of applied feed flow rate and feed pressure of 20 bars (closed symbols) and 25 bars (open symbols), operating temperature ~375 °C (a) Feed mixture of 50% H_2 in N_2; (b) Feed mixture of 30% H_2 in N_2. The dotted line represents the amount of H_2 fed per membrane area

The effect of feed flow rate on the measured H_2 flux is significant for both pressures and feed H_2 content applied, but levels off at high rates as shown in Figure 7. In the case of the 50% H_2 in N_2 feed, a H_2 flux and purity equal to 13.5 $Nm^3 \cdot m^{-2} \cdot h^{-1}$ and 96.9 % is obtained, respectively, at the maximum feed flow rate applied. Under these conditions the HRF equals 63%. This agrees well with the required HRF for one separate membrane stage employed in a sequential non-integrated process design consisting of three shift reaction and membrane separation stages [22]. Three such stages would lead to an overall HRF of 90-95%. At lower feed flow rate the HRF readily approaches values above 95%. However, the obtained H_2 purity decreases because lower absolute H_2 flux values are obtained. At 25 bars and a H_2 feed content of 50%, a H_2 flux and purity equal to 6.3 $Nm^3 \cdot m^{-2} \cdot h^{-1}$ and 93.3 % are obtained at a HRF of 94%. The reduction in H_2 feed content from 50% to 30% results in lower absolute flux values due to lower driving force for permeation, and consequently lower HRF and H_2 purity, which demonstrates the importance of optimal integration of the membrane separation in the pre-combustion process. At the maximum feed flow rate applied, H_2 flux and purity equal to 6.1 $Nm^3 \cdot m^{-2} \cdot h^{-1}$ and 93.1 % is obtained, respectively, at HRF of 66%.

4. Demonstration activities

4.1. Membrane module

A 19-tube hydrogen separation module for the demonstration activity, providing for 2.7 m^2 of active membrane surface area, was designed by Reinertsen AS. The design temperature and pressure of the module is 450 °C and 50 barg, respectively. Specific attention was laid on design concepts to minimise concentration polarization that is

known to reduce the effective H_2 flux through the membranes, especially at high operating pressures and hydrogen recovery factors [20]. Without any internals, the shell-side Reynolds number in the Pd-based membrane modules would be rather small, especially near the feed outlet where the hydrogen has been removed. Thus, using internals such as baffles to enhance mass-transfer and enforce counter-current flow are advantageous. Computational fluid dynamics (CFD) analyses show that both a baffled design and a design based on perforated plates appear to be acceptable from a fluid flow point of view. The baffles and perforated plates generate turbulence for good bulk-to-membrane mass transfer at the shell side and ensure that the flow is predominantly counter-current to the sweep direction. Fig. 8 shows the proposed membrane module for demonstration activities.

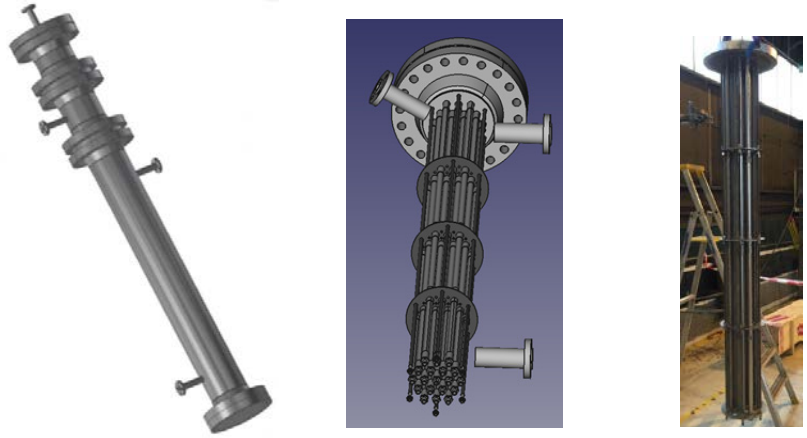

Fig. 8. Membrane module for demonstration activities, (a) outer appearance; (b) baffled design; (c) two full length Pd membrane tubes installed in the module for the first tests.

4.2. Skid construction and testing at Tjeldbergodden

A membrane skid capable of handling up to 2.7 ton per day (200 $Nm^3 \cdot h^{-1}$) synthesis gas slipstream was designed (Fig. 9(a)), constructed, and installed at the Statoil 2500 MTPD methanol synthesis plant in Tjeldbergodden, Norway, for a 12-month field test. The skid has the following possibilities:

- Possibility to control the synthesis gas feed flow rate between 10 and 200 $Nm^3 \cdot h^{-1}$
- Possibility to control the feed pressure between 15 – 31 barg
- Possibility to control the permeate pressure between 2.5 – 15 barg
- Flow measurements on the feed, retentate and permeate streams
- Gas composition measurements by gas chromatography, alternating automatically between the feed, retentate and permeate stream
- Automated start-up and shut down procedures and data logging systems

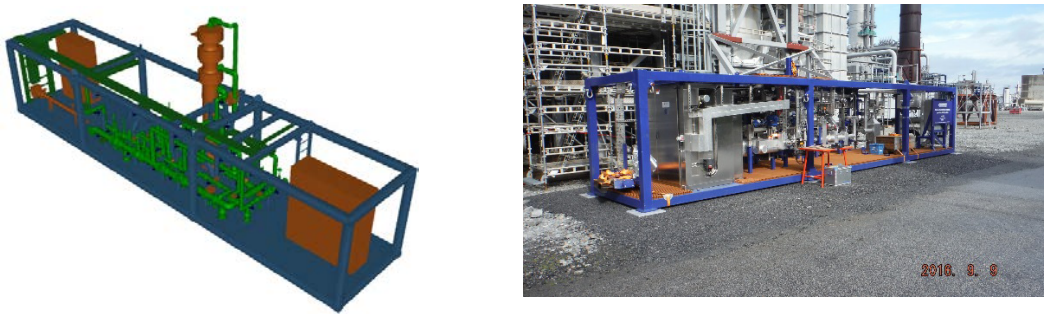

Fig. 9. (a) Design of the membrane skid; (b) skid appearance installed at the Statoil methanol synthesis plant in Tjeldbergodden, Norway.

The skid was transported to Tjeldbergodden in September 2016. The test period is planned for a one-year period until September 2017. Fig. 9(b) shows the skid after the installation at Tjeldbergodden. As the density of the hydrogen-rich gas entering the feed inlet is much lower than the gas leaving the feed side outlet, the membrane module is placed vertically with the feed inlet up due to buoyancy reasons. The skid is currently being commissioned and the first tests with the membrane configuration shown in Fig. 8(c) are scheduled for October 2016.

5. Conclusions

SINTEF has successfully up-scaled the membrane manufacturing process, both in terms of fabrication of large area free-standing Pd-alloy film, semi-automatization of production, and membrane diameter and length. The membrane quality for these enlarged membranes, in terms of a low leakage, agrees well with short lab-scale membranes prepared earlier. The membrane performance is measured as function of feed flow rate and feed pressure in a feed mixture containing 50% H_2. The effect of feed flow rate on the measured H_2 flux is significant, but levels off at high rates. A H_2 flux and purity equal to 13.5 $Nm^3 \cdot m^{-2} \cdot h^{-1}$ and 96.9 % is obtained, respectively, at the maximum feed flow rate applied. Under these conditions the HRF equals 63%. Reinertsen AS has developed a 19-tube hydrogen separation module for the demonstration activity, providing for 2.7 m^2 of active membrane surface area. Additionally, a membrane skid capable of handling up 2.7 ton per day (200 $Nm^3 \cdot h^{-1}$) synthesis gas slipstream was designed, constructed, and installed at the Statoil 2500 MTPD methanol synthesis plant at Tjeldbergodden, Norway, for a 12-month field test starting in October 2016.

Acknowledgements

The financial support from GASSNOVA through the project "CO_2-fangst og hydrogenproduksjon ved bruk av Pd-membraner" (Project no.: 241447) is gratefully acknowledged.

References

[1] Gazzani M, Turi DM, Ghoniem AF, Macchi E, Manzolini G. Techno-economic assessment of two novel feeding systems for a dry-feed gasifier in an IGCC plant with Pd-membranes for CO_2 capture, Int J Greenh Gas Control 2014:25: 62-78.
[2] Gazzani M, Turi DM, Manzolini G. Techno-economic assessment of hydrogen selective membranes for CO_2 capture in integrated gasification combined cycle, Int J Greenh Gas Control 2014:20: 293-309.
[3] Veenstra P, Iyer M, Nijmeijer A, Geuzebroek F, Moene R, Saukaitis J. Integrated Approach to CO_2 Capture: Fuel Gas Decarbonisation, Energy Procedia 2014:63: 2054-9.
[4] Schiebahn S, Riensche E, Weber M, Stolten D. Integration of H_2-Selective Membrane Reactors in the Integrated Gasification Combined Cycle for CO_2 Separation, Chem Eng Technol 2012:35: 555-60.
[5] Atsonios K, Panopoulos KD, Doukelis A, Koumanakos A, Kakaras E. Exergy analysis of a hydrogen fired combined cycle with natural gas reforming and membrane assisted shift reactors for CO_2 capture, Energ Convers Manage 2012:60: 196-203.
[6] Beavis R. The EU FP6 CACHET project - Final results, Energy Procedia 2011:4: 1074-81.
[7] Dijkstra JW, Jansen D, van den Brink RW, Peters TA, Stange M, Bredesen R, Goldbach A, Xu HY, Gottschalk A, Tlatlik S, Doukelis A. Development of hydrogen membrane reactors for CO_2 capture. In: L.I.Eide (editor), Carbon Dioxide Capture and Storage in Deep Geological Formations, CPL Press and BP, 2009, p. 121-133.
[8] Dijkstra JW, Pieterse JAZ, Li H, Boon J, van Delft YC, Raju G, Peppink G, van den Brink RW, Jansen D. Development of membrane reactor technology for power production with pre-combustion CO_2 capture, Energy Procedia 2011:4: 715-22.
[9] Dijkstra JW, Raju G, Peppink G, Jansen D. Techno-economic evaluation of membrane technology for pre-combustion decarbonisation: Water-gas shift versus reforming, Energy Procedia 2011:4: 723-30.
[10] Atsonios KA, Panopoulos KD, Doukelis AF, Koumanakos AK, Morud J, Kakaras E. Natural gas upgrading through hydrogen selective membranes: Application in Carbon Free Combined Cycles, Energy Procedia 2013:37: 914-23.
[11] Jansen D, Dijkstra JW, van den Brink RW, Peters TA, Stange M, Bredesen R, Goldbach A, Xu HY, Gottschalk A, Doukelis A. Hydrogen membrane reactors for CO_2 capture, Energy Procedia 2009:1: 253-60.
[12] Kurokawa H, Shirasaki Y, Yasuda I. Energy-efficient distributed carbon capture in hydrogen production from natural gas, Energy Procedia 2011:4: 674-80.
[13] Carbon sequestration leadership forum. Supporting development of 2nd and 3rd generation carbon capture technologies; mapping technologies and relevant test facilities, 16-12-2015.
[14] Klette H, Bredesen R, Slotfeldt-Ellingsen D, US Patent 20100028703 A1**,** Leak-proof membrane element and method of manufacturing such an element, 4-2-2010.
[15] Bredesen R, Klette H, US Patent 6086729 A**,** Method of manufacturing thin metal membranes, 11-7-2000.
[16] Mejdell AL, Peters TA, Stange M, Venvik HJ, Bredesen R. Performance and application of thin Pd-alloy hydrogen separation membranes in

different configurations, J Taiwan Inst Chem Eng 2009:40: 253-9.
[17] Peters TA, Stange M, Bredesen R. Development of thin Pd-23%Ag/Stainless Stell composite membranes for application in Water Gas Shift membrane reactors. In: L.I.Eide (editor), Carbon Dioxide Capture and Storage in Deep Geological Formations, CPL Press and BP, 2009, p. 135-155.
[18] Peters TA, Tucho WM, Ramachandran A, Stange M, Walmsley JC, Holmestad R, Borg A, Bredesen R. Thin Pd-23%Ag/stainless steel composite membranes: Long-term stability, life-time estimation and post-process characterisation, J Membr Sci 2009:326: 572-81.
[19] Peters TA, Stange M, Bredesen R. On the high pressure performance of thin supported Pd-23%Ag membranes - Evidence of ultrahigh hydrogen flux after air treatment, J Membr Sci 2011:378: 28-34.
[20] Peters TA, Stange M, Klette H, Bredesen R. High pressure performance of thin Pd-23%Ag/stainless steel composite membranes in water gas shift gas mixtures; influence of dilution, mass transfer and surface effects on the hydrogen flux, J Membr Sci 2008:316: 119-27.
[21] Pex PPAC, v. Delft YC. Silica membranes for hydrogen fuel production by membrane water gas shift reaction and development of a mathametical model for a membrane reactor. In: Thomas DC (editor), Carbon dioxide capture for storage in deep geological formations - results from the CO_2 capture project; capture and separation of carbon dioxide from combustion sources, Elsevier, Naperville, 2005, p. 307-319.
[22] Middleton P, Hurst P, Walker G. Grace: Pre-combustion de-carbonisation hydrogen membrane study. In: Thomas DC (editor), Carbon dioxide capture for storage in deep geological formations - results from the CO_2 capture project; capture and separation of carbon dioxide from combustion sources, Elsevier, Naperville, 2005, p. 409-425.